International Symposium
On Turbulence and Shear Flow
Phenomena (TSFP-9)
June 30 - July 3, 2015 Melbourne, Australia



# STRUCTURE OF 3D OFFSET JETS OVER A SURFACE MOUNTED SQUARE RIB

**Shawn P. Clark**
Department of Civil Engineering
University of Manitoba
75A Chancellors Circle, Winnipeg, Manitoba, R3T 5V6, Canada
shawn.clark@umanitoba.ca

**Baafour Nyantekyi-Kwakye**
Department of Mechanical Engineering
University of Manitoba
75A Chancellors Circle, Winnipeg, Manitoba, R3T 5V6, Canada
umnyankt@myumanitoba.ca

**Mohammad S. Rahman**
Department of Mechanical Engineering
University of Manitoba
75A Chancellors Circle, Winnipeg, Manitoba, R3T 5V6, Canada
rahmanms@myumanitoba.ca

**Sarah Boila**
Department of Civil Engineering
University of Manitoba
75A Chancellors Circle, Winnipeg, Manitoba, R3T 5V6, Canada
umboilas@myumanitoba.ca

**Mark F. Tachie**
Department of Mechanical Engineering
University of Manitoba
75A Chancellors Circle, Winnipeg, Manitoba, R3T 5V6, Canada
mark.tachie@umanitoba.ca

## ABSTRACT

An experimental study was conducted to investigate the structures of three-dimensional offset jet flow over a surface mounted square rib using particle image velocimetry. The square rib was mounted at three different streamwise locations, corresponding to the recirculation region, mean reattachment point and developing region. A proper orthogonal decomposition (POD) was used to extract the energetic structures within the flow. The energetic structures contributed proportionately towards the Reynolds shear stress compared to the turbulent kinetic energy. A two-point correlation analysis was performed on the POD modes to examine the structures contained in the various modes. The results show that the large-scale structures within the flow domain were associated with the most energetic modes. The results also showed that the angle of inclination of the hairpin-like vortices within the inner layer of the flow could be approximated with the low order modes (excluding modes 1 and 2) with inclination angles ranging from 9.3° – 9.9°. The integral length scale decreased with increasing number of POD modes. The results revealed that few number of modes can be used to predict the integral length scales of the structures within the flow field.

## INTRODUCTION

The present study is an experimental investigation of three-dimensional (3D) turbulent offset jets over a two-dimensional (2D) square rib attached to the channel floor. Three-dimensional offset jet is a composite shear flow that possesses the characteristics of classical 3D free jets and wall jets. The features of the recirculation and reattachment regions of an offset jet are also akin to those found in separated and reattached shear flows. In view of their unique and complex characteristics, 3D offset jets are a prototypical flow configuration to study the complex flow physics observed in many environmental and engineering applications. Indeed, 3D offset jets are employed in fluid-thermal systems such as fuel injection systems, film cooling technology, heating, ventilation and air condition systems, environmental transport and mixing of effluent in lakes and rivers. Offset jets, chute blocks and end sills are also used in stilling basins for energy dissipation.

In these and many other applications, turbulent transport phenomena such as fluid entrainment and mixing as well as transport of heat and momentum are largely controlled by the large-scale coherent structures embedded within the flows. Therefore, a thorough understanding of the dynamic roles of the large-scale structures is necessary to improve the design of the aforementioned fluid engineering devices and hydraulic structures. While the two limiting cases of a 3D offset jet (i.e., 3D free jet and 3D wall jet) have been studied in detail over the past decades, only a handful of studies were devoted to investigate the characteristics of 3D offset jets (e.g., Nyantekyi-Kwakye et al., 2014; Agelinchaab and Tachie, 2011a, b). These studies investigated the dynamic role of coherent structures in turbulent transport using the two-point correlation technique. Nyantekyi-Kwakye et al. (2014) used the two-point correlation to investigate large-scale structures within the recirculation region for offset jets with offset height ratio ($h/b_o$, where $h$ is the nozzle offset distance and $b_o$ is the nozzle height) ranging from 2 – 8. The spatial extent of the large-scale structures within the recirculation region increased with $h/b_o$. Agelinchaab and Tachie (2011a) performed a particle image velocimetry (PIV) measurement for offset jets with $h/b_o$ ranging from 0.5 – 3.5 at Reynolds numbers of 5000, 10000 and 20000. They reported that larger structures are more dominant in the outer layer of the

flow compared to the inner layer. Within the inner layer of the flow, these structures were inclined at an angle of 11.2° ± 0.6°.

In the present study, a PIV system is used to investigate the flow structures of 3D turbulent offset jet over a square rib attached to the channel floor using the proper orthogonal decomposition (POD) and two-point correlation. The location of the square rib was varied, and the interaction between the separated shear layer generated by the rib and the offset jet was studied.

## EXPERIMENTAL SETUP AND PROCEDURE

The experiments were performed in an open channel with dimensions 2500 mm long and a square cross section of 200 × 200 mm. The side walls as well as the bottom of the test section were made from smooth acrylic to facilitate optical access. The 3D offset jet was generated from a sharp-edged rectangular nozzle with dimensions 8 mm high ($b_o$) and 48 mm wide. A sketch of the experimental set up is shown in Fig. 1, with $x$ and $y$ representing the streamwise and wall-normal distances, respectively. The experiments were conducted for offset height ratio ($h/b_o$) of 2. The tailwater depth, $y_t$, was maintained constant at 116 mm. The bulk velocity, $U_o$, of the flow was 0.95 ms$^{-1}$ yielding a Reynolds number (Re = $(b_oU_o)/\nu$) and Froude number (Fr = $U_o/(gb_o)^{0.5}$) of 7600 and 3.4, respectively, where ν is the kinematic viscosity of water and $g$ is the acceleration due to gravity. A 2D acrylic rib with square cross section of 10 × 10 mm spanning the entire channel width was positioned at $x/b_o$ = 1.25, 3.45 and 6.25 from the nozzle exit which are represented herein as $R1$, $R2$ and $R3$, respectively. Prior to these measurements, a reference experiment was conducted at similar flow conditions but with no rib mounted on the channel floor, where the mean reattachment length was estimated to be $4.4b_o$ (Nyantekyi-Kwakye et al. 2014). Therefore, the three rib locations examined in the present study corresponded to streamwise locations within the recirculation region ($R1$), mean reattachment point ($R2$) and developing region ($R3$).

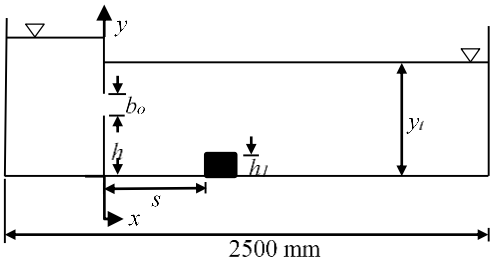


Figure 1. Schematic of experimental setup.

The velocity measurements were performed using a particle image velocimetry (PIV) system over a streamwise range of $0 \le x/b_o \le 80$. The flow was seeded with 10 μm silver coated hollow glass spheres having a specific gravity of 1.4. A New Wave Solo Nd:YAG double-pulsed laser with maximum energy of 120 mJ per pulse at 532 nm wavelength was used to illuminate the flow field. The laser sheet was aligned with the mid-span of the test section for measurements in the $x$–$y$ plane, which coincided with the centre of the nozzle. Scattered light from the tracer particles were captured with a 12-bit FlowSenseEO 4M charge-coupled device camera that has a resolution of 2048 × 2048 pixels and a pixel pitch of 7.4 μm. A camera field of view of 120 × 120 mm was used. The interrogation area size was set to 32 × 32 pixels with 50% overlap in both directions within the $x$–$y$ plane. The instantaneous images were post-processed using the adaptive correlation option of DynamicStudio developed by Dantec Dynamics. Based on initial convergence test, the mean velocities and turbulence statistics were calculated using 4000 instantaneous image pairs.

## RESULTS

### Mean velocity, turbulent kinetic energy and Reynolds shear stress contours

The topology of the flow for the three test cases was qualitatively similar; hence results are only shown for the intermediate test case ($R2$). Contours of the streamwise mean velocity, $U$, approximate turbulent kinetic energy, $k$, and the Reynolds shear stress ($-\overline{uv}$) for $R2$ are shown in Fig. 2 (where $u$ and $v$ are the streamwise and wall-normal fluctuating velocities, respectively). The velocity and length scales used are $U_o$, and $b_o$, respectively. Figure 2(a) shows that the velocity of the discharged jet increased close to the nozzle exit. This phenomenon is attributed to the vena-contracta effect. The increase in $U$ occurred over a streamwise distance of $x^* \le 2.2$ compared to about $x^* \le 4.6$ and $x^* \le 3.4$ for $R1$ and $R3$ (both not shown; $x^* = x/b_o$), respectively. The longer extent for $R1$ was a combination of the vena-contracta effect and the presence of the rib close to the nozzle exit, which caused the flow to accelerate pass it. The $U$ contours the spread of the jet in the wall-normal direction with $x^*$. This is a strong indication of entrainment of ambient fluid. A recirculation region was created underneath the jet upon discharge as a result of an adverse pressure gradient. In the case of $R2$ and $R3$ (not shown), two recirculation regions were formed, one prior to the leading edge of the rib and the second one formed at the trailing edge of the rib. There was however only one recirculation region for $R1$ since the rib was located within the primary recirculation region of the jet. A backflow region was formed within the outer layer of the jet as can be seen from Fig. 2(a).

Figure 2(b) shows the contour plot of the turbulent kinetic energy, $k$ for $R2$. The $k$ was approximated as: $k = 0.75(\overline{u^2}+\overline{v^2})$, since the $w$, the lateral fluctuating velocity, was not measured. The distribution of $k$ revealed that the maximum value occurred close to the nozzle exit for $R1$ (not shown). Changing the rib location from $R1$ to $R2$ and $R3$ shifted the peak farther downstream of the reattachment. The peak value of $k$ occurred at $x^* = 12$ for $R2$ and R$3$ compared to $x^* = 0.5$ for $R1$. Also changing the rib location from $R1$ to $R2$ and $R3$ resulted in a 25% increase in $k$. The high levels of $k$ for $R2$ and $R3$ can be attributed to multiple separations due to the placement of the rib. The turbulent kinetic energy is diffused from the core region of the jet into the inner and outer layers of the flow.

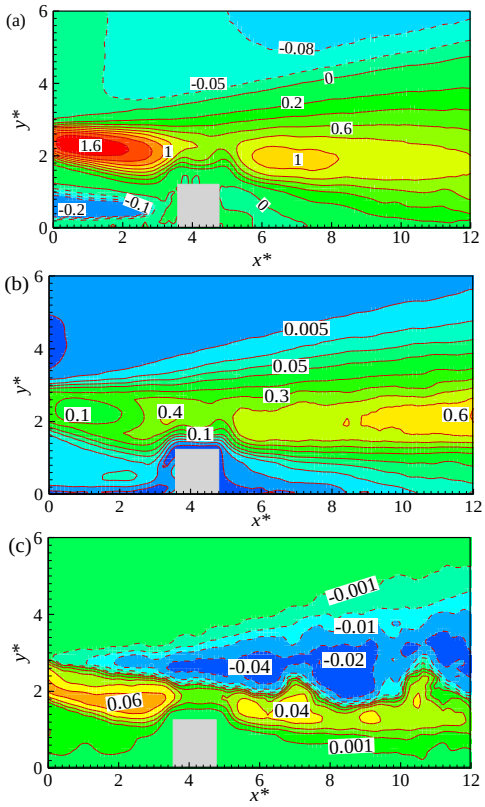


Figure 2. Contour plots of (a) $U$, (b) $k$ and (c) $-\overline{uv}$ ($x^* = x/b_o$; $y^* = y/b_o$).

The distribution of the Reynolds shear stress is shown in Fig. 2(c). The contour depicts an anti-symmetric distribution of $-\overline{uv}$ with positive values closer to the wall and negative values farther away from the wall. The maximum value of $-\overline{uv}$ decreased with streamwise distance and this was qualitatively similar in all three test cases. This occurrence can be partly explained by the mixing and spreading of the developing shear layer. Changing the rib location affected the peak value of $-\overline{uv}$. For example, changing the rib location from $R1$ to $R2$ resulted in a 15% decrease in the maximum value of $-\overline{uv}$. However, the maxima of the Reynolds shear stress increased by 11% for $R3$.

## Proper Orthogonal Decomposition Analysis

A proper orthogonal decomposition (POD) analysis was used in the present study to extract the dominant features and identify coherent structures within the flow field. The snapshot approach proposed by Sirovich (1987) was adopted in the present investigation. This approach is described in detail in previous studies (Meyer et al. 2007) and is not repeated here. The number of snapshots required for convergence of the POD technique was investigated. The results indicate that the 4000 snapshots utilized in the present study were sufficient to allow for the convergence of the result.

Figure 3 shows the fractional and cumulative energy for the first 50 modes for all test cases within three measurement planes. Planes 1, 2 and 4 correspond to flow domain within the recirculation, developing and self-similar regions (defined as the streamwise region where flow quantities do not vary with streamwise distance when the appropriate scaling is applied), respectively. The rate of decay of the fractional energy increased from plane 1 to plane 4. For instance in the case of $R2$, the fractional energy decayed by 93%, 95% and 99% within planes 1, 2 and 4, respectively for the first 50 modes. The fractional energy was larger in plane 4 than in planes 1 and 2. This implies that the low order modes within the self-similar region are more organized and energetic than in the recirculation and developing regions.

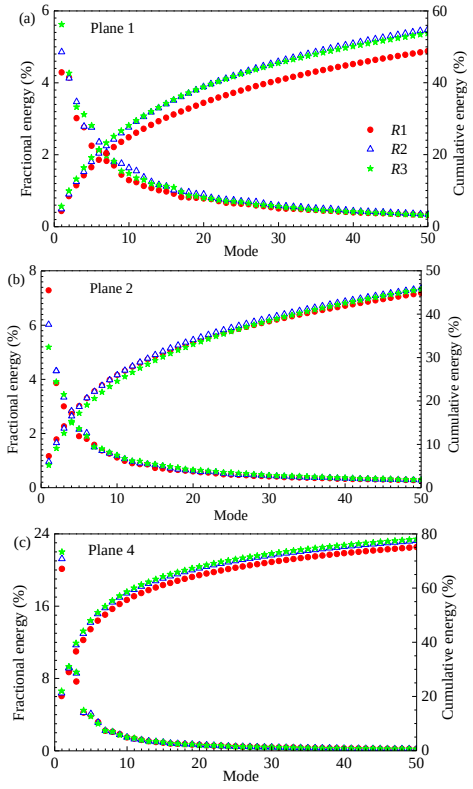


Figure 3. Energy spectra for the measurement planes.

The cumulative energy distribution converged at a slower rate for $R1$ compared to both $R2$ and $R3$ in plane 1.The rib location did not significantly influence the cumulative energy distribution within planes 2 and 4. Since the flow structures are more organized in plane 4, fewer modes were required to capture 50% and 90% of the total energy compared to planes 1 and 2. For instance for $R2$, 38 and 646 modes contributed 50% and 90% of the total energy within plane 1. However, 6 and 293 modes contributed 50% and 90% of the total turbulent kinetic energy, respectively, in plane 4.

Figures 4 and 5 show reconstructed fields for $k$ and $-\overline{uv}$, respectively, for $R2$ using modes 1 and 2 within plane 1. These are compared to their corresponding contours obtained from the ensemble averaged PIV data. Within plane 1, modes 1 and 2 contributed about 17% and 8%, respectively towards the peak value of $k$. Similarly, a contribution of 40% and 35% was made by modes 1 and 2,

respectively, towards the negative peak of $-\overline{uv}$. Within the self-similar region (not shown), mode 1 contributed 33% and 51% towards the turbulent kinetic energy and Reynolds shear stress, respectively. The first 10 modes contributed 47% and 94%, respectively, towards the turbulent kinetic energy and Reynolds shear stress within the self-similar region. This is an indication that the low order modes, which represent the most energetic structures, contributed proportionately to $-\overline{uv}$ than $k$. The present results can be compared to previous measurements in 3D wall jet flows. For example, Agelinchaab and Tachie (2011c) reported that the first 10 modes contributed about 100% towards the Reynolds shear stress within the self-similar region.

The orientation and physical size of the coherent structures embodied in the low order POD modes were also investigated using a two-point correlation analysis. The two-point correlation function was defined at a reference point ($x_r$, $y_r$) between two arbitrary quantities; $a$ and $b$ as:

$$R_{ab} = \overline{a(x_r,y_r)b(x_r+\Delta x,\, y_r+\Delta y)} \big/ a'(x_r,y_r)b'(x_r+\Delta x, y_r+\Delta y),$$

where $a'$ and $b'$ are the root mean square values of $a$ and $b$, respectively. The arbitrary quantities $a$ and $b$ can either be the streamwise or wall-normal fluctuating velocity components. Analysis of the two-point correlation was conducted for modes ranging from 1 to 3500 within the self-similar region of the flow but only contours of 1, 2, 3, 4, 10, 20 and 50 are presented. The results are compared to the ensemble averaged PIV data. The results for $R1$, $R2$ and $R3$ were qualitatively similar and as such only plots for $R2$ are presented. Figure 6 shows the spatial distribution of the streamwise two-point correlation function contour ($R_{uu}$) for the selected modes and ensemble averaged PIV data. The structures presented in Fig. 6 were extracted at $y/y_m$ = 0.5 although the analyses was done all the way into the outer layer of the jet ($y/y_m$ = 2). The two-point correlation analysis revealed that the more energetic modes are indeed associated with the larger structures within the flow. For examples, the largest structure was obtained from the first mode which happens to be the most energetic. The first and second mode exhibited significant structural differences. However, there were no significant structural differences when the number modes were increased. Increasing the number of modes resulted in a decrease in the spatial extents of the structures and also a more distinct inclination of the structures. As the number of modes increased, the structure tends to take the exact shape and orientation of the ensemble PIV data as indicated in Fig. 6e-h. The dynamic role of the less energetic modes in shaping the size of the structures is apparent from Fig. 6.

The angle of inclination of the $R_{uu}$ contours within the inner layer ($\beta$) of the jet represents the average inclination of the hairpin-like vortices. The values of $\beta$ were obtained by fitting ellipses through the farthest points of the various contour levels (0.5–0.9) from the self-correlation peak. The values of $\beta$ estimated from the $R_{uu}$ contours for mode 4 to mode 50 ranged from 9.3° – 9.9° which are in close agreement with $\beta$ = 10.9° estimated from the ensemble averaged PIV data. These values are in agreement with 11°

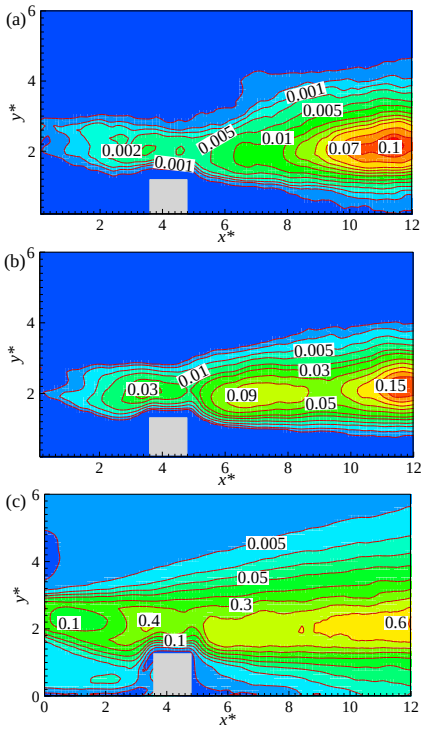


Figure 4. Reconstructed contours of $k$ (a) mode 1, (b) mode 2 and (c) PIV data.

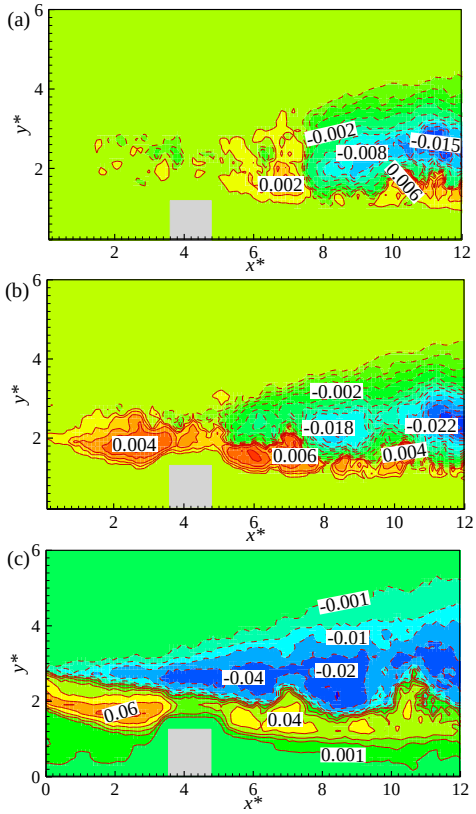


Figure 5. Reconstructed contours of $-\overline{uv}$ (a) mode 1, (b) mode 2 and (c) PIV data.

± 3° reported by Agelinchaab and Tachie (2011c) for 3D wall jet, and also $\beta$ = 10° obtained in turbulent boundary layer flows (Krogstad and Antonia, 1994).

The length scale, $Lx_{uu}$ was estimated as twice the distance from the self-correlation peak to the most downstream location of the 0.5 $R_{uu}$ contour level. Values of $Lx_{uu}$ were estimated at wall-normal locations, $y/y_m$ = 0.5, 1 and 2. The values of $Lx_{uu}$ were normalized by $b_o$ and shown in Fig. 7. As expected, larger values of $Lx_{uu}$ were obtained from the most energetic modes and this was persistent at all three wall-normal locations. Increasing the number of modes resulted in a decrease in the estimated length scale. For example at $y/y_m$ = 0.5, increasing the number of modes from 4 to 5 resulted in a 20% decrease of the estimated length scale. Beyond mode 200, values of $Lx_{uu}$ approached that obtained from the PIV data. Increasing the number of modes beyond 2000 caused the $Lx_{uu}$ value to fall below the obtained value from the PIV data. Studies have shown that the outer layer of 3D offset jet flow is characterized by larger structures compared to the inner layer (Agelinchaab and Tachie, 2011a). However, this was not the case in the present investigation except for the first four modes. Beyond the first four modes, lower values of $Lx_{uu}$ were obtained at $y/y_m$ = 2 (which is within the outer layer of the jet) compared to $y/y_m$ = 0.5 and 1. For example for the first 10 modes, the size of the large-scale structure decreased by about 12% and 33% when $y/y_m$ was changed from 0.5 to 1 and 2, respectively. Similarly, for the ensemble averaged PIV data $Lx_{uu}$ = 5.2, 5 and 4.8 were obtained at $y/y_m$ = 0.5, 1 and 2, respectively. The decrease can be partly explained by the presence of the backflow region within the outer layer of the jet.

## CONCLUSION

A PIV technique was used to investigate the flow structure of 3D offset jet flow over surface mounted square rib. The rib was mounted at three different streamwise locations, 1.25$b_o$, 3.45$b_o$ and 6.25$b_o$ represented herein as $R1$, $R2$ and $R3$, respectively from the nozzle exit. The topology of the flow revealed that the offset jet accelerated upon discharge due to the vena-contracta effect. The distribution of turbulent kinetic energy showed that the energy is diffused from the core region of the jet into both the inner and outer layers of the flow. Analysis from the proper orthogonal decomposition (POD) highlighted the significant contribution of the energetic structures towards the Reynolds shear stress compared to the turbulent kinetic energy. A two-point correlation analysis on the POD modes revealed that the energetic modes are associated with the large-scales structures within the flow. This implies that the large-scale structures control the dynamics of the Reynolds shear stress. The inclination of the hairpin-like vortices within the flow could be estimated using the low order POD modes (except modes 1 and 2 in the present investigation) with inclination values ranging from 9.3° – 9.9°. These values are in good agreement with 10.9° for the ensemble averaged PIV data. The current inclination angles are also in good agreement with values reported for boundary layer flows. Larger integral length scales were estimated for the first few modes. The length scale decreased when the number of POD modes was increased.

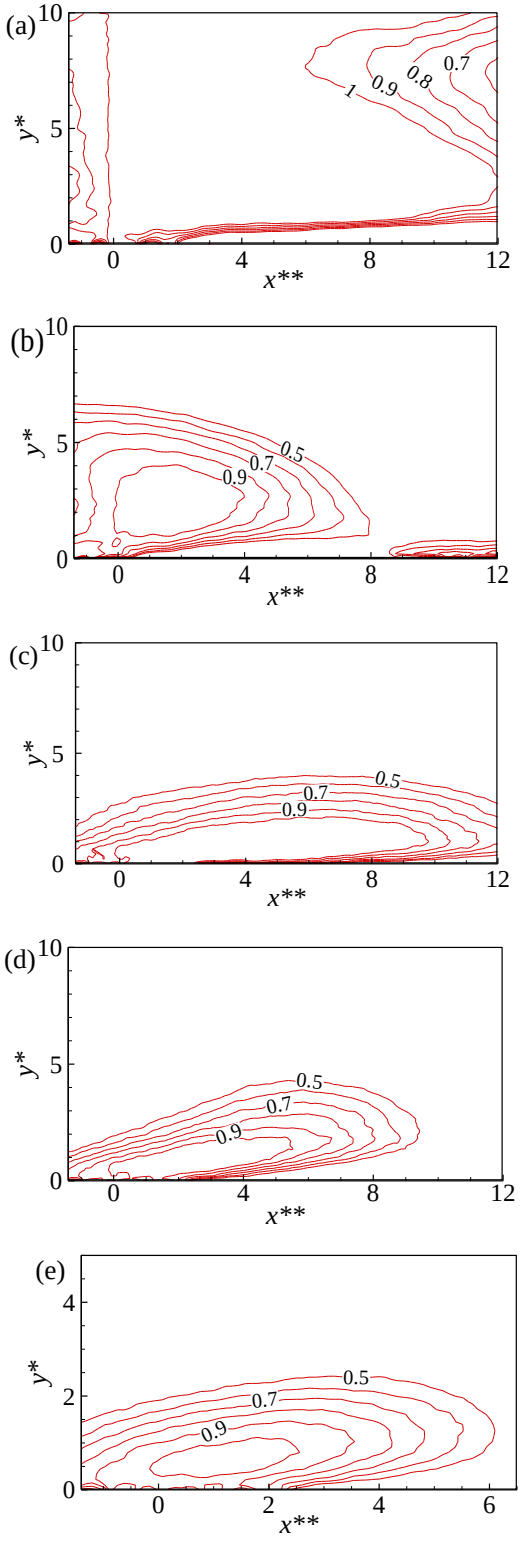

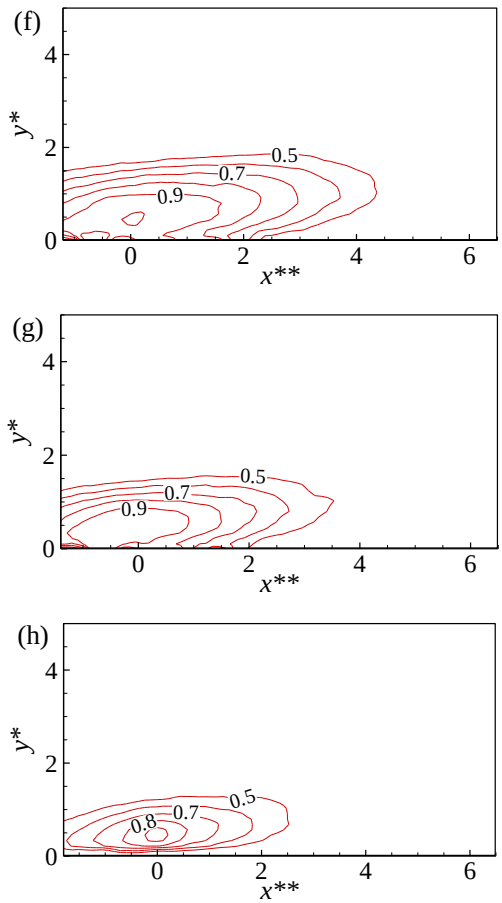


Figure 6. Contours plots of the $R_{uu}$ correlation for (a) mode 1, (b) mode 2, (c) mode 3, (d) mode 4, (e) mode 10, (f) mode 20, (g) mode 50 and (h) ensemble averaged PIV data, (where $x^{**} = (x - x_r)/b_o$).

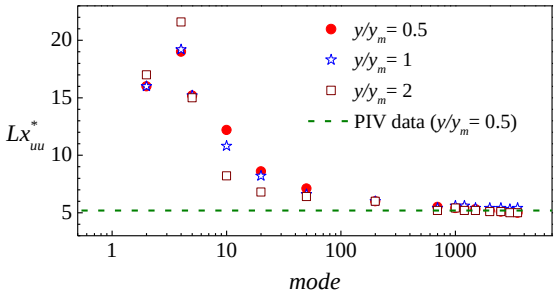


Figure 7. Estimated integral length scales for the POD modes at different wall-normal locations.

## REFERENCE


Agelinchaab, M., and Tachie, M. F., 2011a, "Characteristics and structure of turbulent 3D offset jets", *International Journal of Heat and Fluids Flow*, Vol. 32, pp. 608-620.

Agelinchaab, M., and Tachie, M. F., 2011b, "Characteristics of turbulent three-dimensional offset jets", *Journal of Fluids Engineering*, Vol. 133.

Agelinchaab, M., and Tachie, M. F., 2011c, "Characteristics of turbulent three-dimensional wall jets", *Journal of Fluids Engineering*, Vol. 133, pp. 1-12.

Krogstad, P. A., and Antonia, R. A., 1994, "Structure of turbulent boundary layers on smooth and rough walls", Journal of Fluid Mechanics, Vol. 277, pp. 1-21.

Meyer, E. K., Pedersen, J. M., and Ozcan, O., 2007, "A turbulent jet in crossflow analysed with proper orthogonal decomposition", *Journal of Fluid Mechanics*, Vol. 583, pp. 199-227.

Nyantekyi-Kwakye, B., Clark, S., Tachie, M. F., Malenchak, J., and Muluye, G., 2014, "Flow characteristics within the recirculation region of 3D turbulent offset jet", *Journal of Hydraulic Research*, pp. 1-13.

Sirovich, L., 1987, "Turbulence and the dynamics of coherent structures, Part 1: coherent structures", *Quarterly of Applied Mathematics*, Vol. 45, pp. 561-571.